Laser cooling of trapped ions with polarization gradients

J. I. Cirac
Departamento de Fisica Aplicada, Facultad de Quimicas, Universidad de Castilla–La Mancha, 13071 Ciudad Real, Spain

R. Blatt
Institut für Laser-Physik, Jungiusstrasse 9, D-2000, Hamburg 36, Germany

A. S. Parkins, and P. Zoller
Joint Institute for Laboratory Astrophysics and Department of Physics, University of Colorado, Boulder, Colorado 80309-0440
(Received 8 April 1993)

Laser cooling of a single trapped ion with Zeeman substructure below the Doppler limit is considered theoretically. The laser field consists of two counterpropagating beams linearly polarized in different directions, and the internal atomic transition is $J_g = \frac{1}{2} \rightarrow J_e = \frac{3}{2}$. The ion is assumed to be localized to spatial dimensions smaller than the optical wavelength (Lamb-Dicke limit) and placed at a specific position with respect to the laser beams. Under the assumption that the rate for optical pumping between the atomic ground states defines the smallest time constant in the system, analytic expressions for the final energy and the cooling rates are derived, with both a semiclassical and a full quantum treatment. The results show that laser cooling of a trapped ion using polarization gradients leads to very low energies. These energies are insensitive to the precise localization of the ion with respect to the lasers, the angle between the direction of the polarizations of the laser beams, and the detuning of the cooling laser.

PACS number(s): 32.80.Pj

I. INTRODUCTION

During the past years cooling and trapping of atoms and ions have become a technique of increasing importance in the field of quantum optics and precision spectroscopy [1–4]. Although laser cooling of trapped ions has been known and applied for some time now, it was not until the development of very efficient cooling techniques for neutral atoms [5] that laser cooling of trapped ions was revisited and shown to offer similar possibilities for achieving lower temperatures and higher cooling rates than those obtained so far [6,7]. For neutral atoms, these cooling concepts are making use of the high forces obtainable with intensity gradient and polarization gradient fields [8–11].

The theory of laser cooling of single ions trapped in harmonic potentials was essentially developed during the past decade by Wineland and Itano [12], and by Stenholm and co-workers [13–15]. Generally, one distinguishes cases where the trap frequency ν is larger and smaller than the natural linewidth Γ of the transition that is used for optical cooling. Experimentally, $\Gamma > \nu$ is most often realized (i.e., the so called weak-confinement or weak-binding case), for which the final temperature of the cooling process is given by $k_b T = \hbar\Gamma/2$ (Doppler limit), where k_B is the Boltzmann constant. In this case, the final quantum state of the ion in the trap is a thermal state, described by a Boltzmann distribution with a mean occupation number $\langle n \rangle$ that is approximately given by the ratio $\Gamma/(2\nu)$. For experiments in quantum optics and for precision experiments, which usually require a minimum energy, it is, of course, desirable to reach a quantum number as low as possible. This can be achieved for a single trapped ion when $\Gamma < \nu$ (i.e., the so-called strong-confinement or strong-binding case). In this case, the ion develops motional sidebands such that absorption on a sideband becomes possible and optical pumping transfers the trapped ion to the lowest quantum state in the trap. However, for allowed dipole transitions with Γ on the order of tenths of MHz, this is difficult to achieve in experiments and so far only weakly allowed transitions [yielding $\Gamma < \nu$] could be used for sideband cooling [16].

More recently, laser cooling of trapped ions with *intensity* gradient configurations (standing-wave fields) was shown to be advantageous for reaching lower temperatures and higher cooling rates. Since a single laser-cooled ion in a Paul trap can be localized to spatial dimensions much smaller than an optical wavelength (Lamb-Dicke limit), it is possible to place the ion at any position of a standing laser wave. In particular, it has been shown that placing the ion at the node of a standing wave leads to very high cooling rates and the final energy is independent of the applied Rabi frequency [7]. However, for the weak-binding case, which is of experimental importance, laser cooling at the node of a standing wave reduces the final energy only by a factor of about 2 compared to the traveling-wave case. It has also been shown that positioning an ion at the point of a standing wave's steepest gradient allows one to use the Sisyphus cooling concept, as was successfully applied to neutral atoms [8]. The Sisyphus effect is based on the fact that because of the time lag due to optical pumping between two atomic levels, an atom moving slowly in a spatially periodic light field is always climbing potential hills, transforming part of its kinetic energy into potential energy. For two-level

ions the resulting temperature is always larger than the Doppler limit [7]. However, for three-level systems temperatures below the Doppler limit have been predicted [6,7,15].

Here we investigate laser cooling of a single trapped ion with optical transition $J_g = 1/2 \rightarrow J_e = 3/2$ in a laser configuration yielding *polarization* gradients. The ion is assumed to be localized at a specific position with respect to the lasers, i.e., all calculations are performed in the Lamb–Dicke limit. Using standard arguments [6], it is possible to derive analytic expressions for the final energy and the cooling rates in the semiclassical limit under the assumption that the rate for optical pumping between the ground states $\Gamma_{\pm\rightarrow\mp}$ defines the smallest time constant in the system and in the weak-confinement limit, i.e., if the inequality $\Gamma_{\pm\rightarrow\mp} < \nu < \Gamma$, $|\Delta|$ holds (Δ is the detuning between the laser and the transition frequencies). A full quantum treatment of the problem is performed and is analytically reduced to the expressions found under the assumptions for the time scales stated above. As the results show, laser cooling of a trapped ion using polarization gradients leads to final quantum numbers $\langle n\rangle \approx 1$, that is, to final energies $E = \hbar\nu(\langle n\rangle + 1/2) \ll \hbar\Gamma/2$. We will explain these results in terms of the Sisyphus effect, in analogy to the free-atom case. However, it is worth noting that for a single trapped ion that can be precisely localized, we can choose the position of the ion where cooling is optimum, which is not possible with free atoms. Nevertheless, as it turns out, the cooling results are quite insensitive to the precise localization of the ion and as a function of the laser detuning. Thus, for weak confinement, laser cooling with polarization gradients seems superior to other cooling techniques in traps, such as Doppler cooling, cooling at the node of a standing wave, or even Sisyphus cooling with pure intensity gradients.

The paper is organized as follows: in Sec. II we present the model and write the parameters and the interaction potential. A qualitative consideration of the Sisyphus cooling concept including polarization gradients is given in the first part of Sec. III, and in the second part cooling rates and final temperatures are calculated with arguments given by Wineland, Dalibard, and Cohen-Tannoudji [6]. Section IV comprises a full quantum treatment of the problem, which is analytically reduced and compared with the results of Sec. III. Finally, we present numerical results for cooling rates and final energies as a function of the Rabi frequency and the detuning in Sec. V.

II. MODEL

We consider laser cooling of an ion trapped in a one-dimensional harmonic potential of frequency ν,

$$V_{\mathrm{HP}} = \frac{1}{2}M\nu^2 z^2. \tag{1}$$

We assume that the internal structure of the ion is excited by two counterpropagating laser beams, linearly polarized, with the corresponding electric fields forming an angle θ. The total electric field can be written as

$$\mathbf{E}(z,t) = E_0[\mathbf{e}_1 e^{-i(\omega_L t - k_L z - \phi)} + \mathbf{e}_2 e^{-i(\omega_L t + k_L z + \phi)} + c.c.]. \tag{2}$$

Here ϕ is a laser phase that shifts the laser relative to the center of the trap potential ($z = 0$), $k_L = \omega_L/c = 2\pi/\lambda$ is the laser wave-vector,

$$\mathbf{e}_1 = \cos\left[\frac{\theta}{2}\right]\mathbf{e}_x + \sin\left[\frac{\theta}{2}\right]\mathbf{e}_y, \tag{3a}$$

$$\mathbf{e}_2 = \cos\left[\frac{\theta}{2}\right]\mathbf{e}_x - \sin\left[\frac{\theta}{2}\right]\mathbf{e}_y, \tag{3b}$$

and $\mathbf{e}_x$ and $\mathbf{e}_y$ are unitary vectors in the x and y directions, respectively. Note that for $\theta = 0, \pi$, this electric field reduces to a linearly polarized standing wave. For $\theta = \pi/2$, on the other hand, we have a standing-wave field with polarization gradient but constant intensity (the so-called lin $\perp$ lin laser configuration). In this case the ion located at $z \approx 0$ sees $\sigma^{\pm}$-polarized light for the phase $\phi = \pm\pi/4 + n\pi$, and linear-polarized light for $\phi = n\pi/2$ with $n = 0, \pm 1, \ldots$.

The laser beams excite a $J_g = 1/2 \longrightarrow J_e = 3/2$ transition of frequency ω_0, as shown in Fig. 1, where the laser-induced couplings are indicated by arrows. Defining

$$\varphi_{\pm} = \frac{\theta}{2} \pm \phi, \tag{4}$$

we find the dipole potential for this interaction in a frame rotating at the laser frequency is given by (we set $\hbar = 1$ in the following)

$$V_{\mathrm{dip}}(z) = \frac{\Omega}{\sqrt{2}}\cos(kz + \varphi_+)\left[|e_{3/2}\rangle\langle g_{1/2}| + \frac{1}{\sqrt{3}}|e_{1/2}\rangle\langle g_{-1/2}|\right] - \frac{\Omega}{\sqrt{2}}\cos(kz - \varphi_-)\left[|e_{-3/2}\rangle\langle g_{-1/2}| + \frac{1}{\sqrt{3}}|e_{-1/2}\rangle\langle g_{1/2}|\right] + \mathrm{c.c.}, \tag{5}$$

where Ω is the Rabi frequency of this interaction. This configuration was first discussed by Dalibard and Cohen-Tannoudji in the context of laser cooling of neutral atoms ($\theta = \pi/2$) [9].

In the following we will be interested in the Lamb-Dicke limit, where the ion is well localized to a spatial dimension smaller than the optical wavelength ($k_L z \ll 1$). This condition can also be expressed as $\eta \ll 1$, where

$$\eta = k_L/\sqrt{2M\nu} \tag{6}$$

is the so-called Lamb–Dicke parameter.

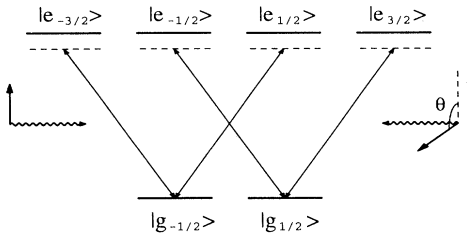

FIG. 1. Level scheme and arrangement of optical waves for polarization gradient cooling.

III. SEMICLASSICAL TREATMENT

In this section we derive a simple formula for the cooling rate and the final energy reached by the ion at the end of the cooling process, using semiclassical arguments, i.e., considering the motional parameters (position and momentum) classically. We also give a qualitative explanation of laser cooling in terms of the Sisyphus effect.

An important parameter in the laser-ion interaction is the saturation parameter s, defined as

$$s = \frac{\Omega^2/2}{\Delta^2 + \frac{\Gamma^2}{4}}, \tag{7}$$

where $\Delta = \omega_L - \omega_0$ is the laser-atomic frequency detuning, and Γ is the spontaneous decay rate. Here we are interested in the low-excitation regime $s \ll 1$. In this case, the excited atomic levels can be adiabatically eliminated, and the internal atomic dynamics can be understood in terms of Raman transitions between the ground levels $|g_{1/2}\rangle$ and $|g_{-1/2}\rangle$. An important point is that the transition rates between these levels depend on the position z, and are different,

$$\Gamma_{+\to-}(z) = \Gamma' \cos^2(k_L z - \varphi_-), \tag{8a}$$

$$\Gamma_{-\to+}(z) = \Gamma' \cos^2(k_L z + \varphi_+), \tag{8b}$$

where $\Gamma_{\pm\to\mp}$ denotes the transition rate from $|g_{\pm 1/2}\rangle$ to $|g_{\mp 1/2}\rangle$, and $\Gamma' = 2/9\ \Gamma s$. Moreover, due to the different Clebsch-Gordan coefficients for the various transitions $g_m \to e_n$, and due to the change of polarization with z, the ac-Stark shifts, U_+ in the level $|g_{1/2}\rangle$ and U_- in $|g_{-1/2}\rangle$, form an oscillating pattern of optical bipotentials (see Fig. 2, upper part)

$$U_\pm = \frac{2}{3}\Delta s + \frac{1}{3}\Delta s[2\cos(\theta)\cos(2k_L z + 2\phi) \mp \sin(\theta)\sin(2k_L z + 2\phi)]. \tag{9}$$

Note that the difference between these potentials is proportional to $\sin(\theta)$. Thus, for $\theta = 0$ (which correponds to a standing-wave configuration) they coincide and for $\theta = \pi/2$ they alternate in space.

The total spatial potential seen by the ion is $V_\pm = V_{tp} + U_\pm$, depending on whether the ion is in $|g_{1/2}\rangle$ or in $|g_{-1/2}\rangle$. Since we are interested in the Lamb-Dicke limit, we can expand $U_\pm$ up to first order in $k_L z$, obtaining for $V_\pm$

$$V_\pm(z) = \frac{1}{2}M\nu^2(z - z_\pm)^2 + c_\pm, \tag{10}$$

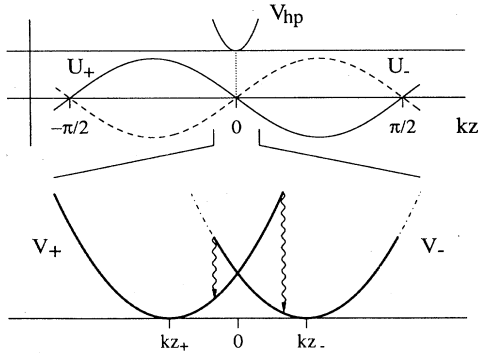

FIG. 2. Harmonic trap potential $V_{\rm HP}$ and optical bipotential $U_\pm$ in the wave pattern for polarization gradient cooling result in the shifted potentials $V_\pm$ centered at kz_+ and kz_-. Parameters are $\theta = \pi/2$ and $\phi = 0$ (lin $\perp$ lin configuration). We assume $\Delta < 0$ so that $z_+ < 0 < z_-$.

where

$$k_L z_\pm = \frac{4}{3}\eta^2\frac{\Delta s}{\nu}[2\cos(\theta)\sin(2\phi) \pm \sin(\theta)\cos(2\phi)], \tag{11}$$

and

$$c_\pm = \mp\frac{1}{3}\Delta s \sin(\theta)\sin(2\phi). \tag{12}$$

Note that, as a result of the ac-Stark effect, for given ϕ and θ the potential V_+ (V_-) is displaced along the z axis by z_+ (z_-), and along the potential axis by c_+ (c_-). For $\phi = 0, \pi/2$ both potentials are only shifted along the z axis, while for $\phi = \pi/4, 3\pi/4$ they are only shifted along the potential axis, i.e., both potentials are centered at the same position. In Fig. 2 (lower part) we have plotted V_+ and V_- for $\theta = \pi/2$ and $\phi = 0$. In this figure we assumed $\Delta < 0$, so that $z_+ < 0 < z_-$ (the condition $\Delta < 0$ is required for cooling as discussed in Sec. III B).

A. Qualitative explanation of the cooling

A qualitative explanation of cooling can be given by the following reasoning: let us assume that

$$\Gamma_{\pm\to\mp} \ll \nu \ll \Gamma \ll |\Delta|, \tag{13}$$

and that we have red detuning $\Delta < 0$. For the sake of simplicity we will also assume $\theta = \pi/2$ (lin $\perp$ lin configuration) and $\phi = 0$. When the ion is in the state $|g_{1/2}\rangle$, that is, oscillating in the potential V_+, it will be transferred after a time of the order of $\Gamma^{-1}_{+\to-}$ to $|g_{-1/2}\rangle$ via a Raman transition. According to (8a) this transition will

preferably take place for $z > 0$ (as shown by a wavy curve in Fig. 2). Since the ion does not change its position significantly during the transition time, the potential energy of the ion decreases in the process. Then, after oscillating in the potential V_- for a time of the order of $\Gamma^{-1}_{-\to+}$ it will be transferred back to V_+, but now, preferably when $z < 0$. Again, in this process the potential energy will decrease. As a result, the ion switches from one potential to the other, always diminishing its potential energy and, since in each of the potentials the total external energy (kinetic+potential) is conserved, the total energy of the ion decreases. This is analogous to the Sisyphus effect found for neutral atoms [8,9]. Note that for other values of θ and ϕ, similar arguments can be developed.

B. Cooling rate and final temperature

To determine the cooling rate and the final temperature reached by the ion in polarization gradient cooling, we will use the arguments similar to those given by Wineland, Dalibard, and Cohen-Tannoudji [6].

After a time $t > \Gamma^{-1}$, the variation of the external energy can be expressed by the equation

$$\begin{aligned}\dot{E} = {} & \rho^{\mathrm{SS}}(g_{1/2}, g_{1/2})\langle \Gamma_{+\to-}(z)[V_-(z) - V_+(z)]\rangle_+ \\ & + \rho^{\mathrm{SS}}(g_{-1/2}, g_{-1/2})\langle \Gamma_{-\to+}(z)[V_+(z) - V_-(z)]\rangle_- \\ & + 2R. \end{aligned} \tag{14}$$

Here $\rho^{\mathrm{SS}}(g_{1/2}, g_{1/2})$ and $\rho^{\mathrm{SS}}(g_{-1/2}, g_{-1/2})$ are the averaged steady-state population of the ground levels and $\langle\rangle_\pm$ indicates an average over one period of the oscillation in the potentials $V_\pm$. The first and second terms in this equation give the average rates at which the potential energy changes due to transitions from $|g_{1/2}\rangle$ to $|g_{-1/2}\rangle$, and from $|g_{-1/2}\rangle$ to $|g_{1/2}\rangle$, respectively, and include the cooling and heating due to these changes. The $2R$ term gives the diffusion due to the random momentum of the scattered photons and to the fluctuations of the dipole force.

For $\theta = \pi/2$ and $\phi = 0$, it can be shown by symmetry arguments that $\rho^{\mathrm{SS}}(g_{1/2}, g_{1/2}) = \rho^{\mathrm{SS}}(g_{-1/2}, g_{-1/2}) = 1/2 + o(\eta)$, and that the second term in (14) gives the same contribution as the first one. Hence, we obtain

$$\begin{aligned}\dot{E} &= \langle \Gamma_{+\to-}(z)[V_-(z) - V_+(z)]\rangle_+ + 2R \\ &= \frac{2}{3}\Gamma' \Delta s[\langle k_L z\rangle_+ + 2\langle (k_L z)^2\rangle_+] + 2R, \end{aligned} \tag{15}$$

where for the last line we have expanded in $k_L z$ up to second order. On the other hand, using (11) we have

$$\begin{aligned}\langle (k_L z)^2\rangle_+ &= \langle [k_L(z - z_+)]^2\rangle_+ + (k_L z_+)^2 \\ &= 2\eta^2 E/\nu + o(\eta^4), \end{aligned} \tag{16}$$

where we have used equipartition of the energy in the potential V_+, i.e., $E = M\nu^2\langle [k_L(z - z_+)]^2\rangle_+$. Hence, we find

$$\langle \Gamma_{+\to-}(z)[V_-(z) - V_+(z)]\rangle_+ = \frac{8}{3}\eta^2 \frac{\Gamma' \Delta s}{\nu}\left[\frac{1}{3}\Delta s + E\right]. \tag{17}$$

The diffusion constant R has two contributions,

$$R = R_{\mathrm{vac}} + R_{\mathrm{dip}}, \tag{18}$$

where R_{vac} gives the contribution due to the random direction of the spontaneously emitted photons, and R_{dip} accounts for the fluctuations of the dipole force. In the limit $s \ll 1$ considered here, we can calculate these diffusion constants by independently adding the diffusion in each driven transition $g_i \to e_j$, as derived by Gordon and Ashkin [17]. Using their results, we have

$$R_{\mathrm{vac}} = \frac{k_L^2}{2M}\frac{\Gamma}{4} s \cos^2(\pi/4)\left(2\alpha_1 + 2\frac{1}{3}\left[\frac{1}{3}\alpha_1 + \frac{2}{3}\alpha_2\right]\right), \tag{19}$$

where we have included the factors $\alpha_1 = 2/5$ and $\alpha_2 = 1/5$, which account for the different projections of the momentum of the spontaneously emitted photons in the z direction due to the transitions $|g_{\pm1/2}\rangle \to |e_{\pm3/2}\rangle$ and $|g_{\pm1/2}\rangle \to |e_{\mp1/2}\rangle$, respectively. Substituting these values and using (6), we get

$$R_{\mathrm{vac}} = \frac{11}{90}\eta^2 s \Gamma \nu. \tag{20}$$

For R_{dip} we obtain

$$\begin{aligned} R_{\mathrm{dip}} &= \frac{k_L^2}{2M}\frac{\Gamma}{4} s \sin^2(\pi/4)(1 + 1 + 1/3 + 1/3) \\ &= \frac{1}{3}\eta^2 s \Gamma \nu. \end{aligned} \tag{21}$$

Finally, inserting (17), (20), and (21) in Eq. (15) we obtain

$$\dot{E} = -W(E - E_0), \tag{22}$$

where the cooling rate W is given by

$$W = 8\eta^2 \Gamma' \xi, \tag{23}$$

and the energy at the end of the cooling process is

$$E_0 = \nu\left[\xi + \frac{41}{80\xi}\right], \tag{24}$$

with

$$\xi = -\frac{1}{3}\frac{\Delta s}{\nu}. \tag{25}$$

We note that polarization gradient cooling (with $\theta = \pi/2$ and $\phi = 0$) in a $J_g = 1/2 \to J_e = 3/2$ configuration requires $\Delta < 0$ ($\xi > 0$).

IV. QUANTUM TREATMENT

In this section we employ the method introduced in Ref. [7] to calculate the cooling rate and final temperature, using a full quantum treatment. This method is valid for all sets of parameter values. We will show that the results reduce to those found with the semiclassical treatment (Sec. III) in the appropriate limits.

According to Ref. [7] the (quantum) dynamics of a laser-cooled trapped ion in the Lamb-Dicke limit is determined by the coefficients $A_\pm$, defined as

$$A_\pm = 2\,\mathrm{Re}[S(\mp\nu)] + 2D. \tag{26}$$

The $A_\pm$ are proportional to transition rates between the harmonic-oscillator states. In Ref. [7] we have shown that in terms of the coefficients $A_\pm$ the rate at which the energy is damped (cooling rate) is given by

$$W = A_- - A_+, \tag{27}$$

and the final energy can be written as

$$E^{SS} = \nu\left[\langle n\rangle + \frac{1}{2}\right], \tag{28}$$

where

$$\langle n\rangle = \frac{A_+}{A_- - A_+} \tag{29}$$

is the mean occupation number of the harmonic oscillator in steady state.

In the present case we have

$$S(\nu) = \eta^2 \int_o^\infty dt\, e^{i\nu t}\langle F(t)F(0)\rangle_{SS}, \tag{30}$$

which is the Fourier transform of the correlation function of the force operator F (at $z = 0$),

$$F = -\frac{1}{k_L}\frac{dV_{dip}}{dz}\bigg|_{z=0}$$
$$= \frac{\Omega}{\sqrt{2}}\sin(\varphi_+)\left[|e_{3/2}\rangle\langle g_{1/2}| + \frac{1}{\sqrt{3}}|e_{1/2}\rangle\langle g_{-1/2}|\right] + \frac{\Omega}{\sqrt{2}}\sin(\varphi_-)\left[|e_{-3/2}\rangle\langle g_{-1/2}| + \frac{1}{\sqrt{3}}|e_{-1/2}\rangle\langle g_{1/2}|\right] + \text{H.c.} \tag{31}$$

The subscript SS stands for steady state. The second term in Eq. (26) is a diffusion constant,

$$D = \eta^2\frac{\Gamma}{2}[\alpha_1[\rho^{SS}(e_{3/2},e_{3/2}) + \rho^{SS}(e_{-3/2},e_{-3/2})] + (1/3\alpha_1 + 2/3\alpha_2)[\rho^{SS}(e_{1/2},e_{1/2}) + \rho^{SS}(e_{-1/2},e_{-1/2})]], \tag{32}$$

with $\alpha_1 = 2/5$ and $\alpha_2 = 1/5$. Both (30) and (32) can be calculated with the optical Bloch equations for an atom at rest (at $z = 0$), and with the help of the quantum regression theorem. In Sec. IV A below we give approximate analytical solutions of these equations. The plots of this paper as discussed in Sec. V are based on (exact) numerical solutions of these equations.

A. Analytic calculation

In this section we are interested in the derivation of a simple formula in the limits

$$s \ll 1, \tag{33a}$$
$$\nu \ll \Gamma, \Delta. \tag{33b}$$

Denoting

$$R(\alpha,\beta) = \langle A_{\alpha,\beta}(t)F(0)\rangle, \tag{34}$$

with $A_{\alpha,\beta}(0) = |\alpha\rangle\langle\beta|$ (α and β are atomic labels), and

$$\tilde{R}(\alpha,\beta) = \int_0^\infty dt\, e^{i\nu t}R(\alpha,\beta), \tag{35}$$

we can write

$$S(\nu) = \eta^2\frac{\Omega}{\sqrt{2}}\Bigg(\sin(\varphi_+)\left[\tilde{R}(e_{3/2},g_{1/2}) + \tilde{R}(g_{1/2},e_{3/2}) + \frac{1}{\sqrt{3}}\tilde{R}(e_{1/2},g_{-1/2}) + \frac{1}{\sqrt{3}}\tilde{R}(g_{-1/2},e_{1/2})\right]$$
$$+ \sin(\varphi_-)\left[\tilde{R}(e_{-3/2},g_{-1/2}) + \tilde{R}(g_{-1/2},e_{-3/2}) + \frac{1}{\sqrt{3}}\tilde{R}(e_{-1/2},g_{1/2}) + \frac{1}{\sqrt{3}}\tilde{R}(g_{1/2},e_{-1/2})\right] \tag{36}$$

The quantum regression theorem states that $R(\alpha,\beta)$ satisfies the same equation as $\rho(\alpha,\beta)$. Hence, to determine $S(\nu)$ we need the optical Bloch equations for the optical coherences $\rho(e_i,g_j)$. For example, we have for $\rho(e_{3/2},g_{1/2})$

$$\dot{\rho}(e_{3/2},g_{1/2}) = \left[i\Delta - \frac{\Gamma}{2}\right]\rho(e_{3/2},g_{1/2}) - i\frac{\Omega}{\sqrt{6}}\cos(\varphi_-)\rho(e_{3/2},e_{-1/2}) - i\frac{\Omega}{\sqrt{2}}\cos(\varphi_+)[\rho(g_{1/2},g_{1/2}) - \rho(e_{3/2},e_{3/2})]. \tag{37}$$

This equation can be simpified when the condition (33a) is taken into account. In this case, after a time $t \gg \Gamma^{-1}$, the population of the excited levels is negligible compared to the populations of the ground levels, resulting in

$$\dot{\rho}(e_{3/2},g_{1/2}) = \left[i\Delta - \frac{\Gamma}{2}\right]\rho(e_{3/2},g_{1/2}) - i\frac{\Omega}{\sqrt{2}}\cos(\varphi_+)\rho(g_{1/2},g_{1/2}). \tag{38}$$

Starting from this equation we have the following.

(i) In steady state,

$$\rho^{\rm SS}(e_{3/2},g_{1/2}) = \frac{\Omega/\sqrt{2}}{\Delta + i\frac{\Gamma}{2}}\cos(\varphi_+)\rho^{\rm SS}(g_{1/2},g_{1/2}). \tag{39}$$

(ii) Using the quantum regression theorem,

$$\begin{aligned}\tilde{R}(e_{3/2},g_{1/2}) &= \frac{1}{\frac{\Gamma}{2} - i(\Delta+\nu)}\left[R^0(e_{3/2},g_{1/2}) - i\frac{\Omega}{\sqrt{2}}\cos(\varphi_+)\tilde{R}(g_{1/2},g_{1/2})\right] \\ &\simeq \frac{1}{\frac{\Gamma}{2} - i\Delta}\left[R^0(e_{3/2},g_{1/2}) - i\frac{\Omega}{\sqrt{2}}\cos(\varphi_+)\tilde{R}(g_{1/2},g_{1/2})\right],\end{aligned} \tag{40}$$

where in the last line we have used (33b) (i.e., $\Delta - \nu \simeq \Delta$). On the other hand, according to the definition (34), we have for the initial condition $R^0(e_{3/2},g_{1/2}) = \frac{\Omega}{\sqrt{2}}\sin[\varphi_+]\,\rho^{\rm SS}(g_{1/2},g_{1/2})$. Inserting this in (40) we obtain

$$\tilde{R}(e_{3/2},g_{1/2}) = \frac{\Omega/\sqrt{2}}{\frac{\Gamma}{2} - i\Delta}[\sin(\varphi_+)\rho^{\rm SS}(g_{1/2},g_{1/2}) - i\cos(\varphi_+)\tilde{R}(g_{1/2},g_{1/2}] \tag{41}$$

Performing a similar analysis with the rest of the optical coherences, we see that Eq. (36) becomes

$$\begin{aligned}{\rm Re}[S(\nu)] = \eta^2\frac{\Gamma}{2}s\Bigg(&\rho^{\rm SS}(g_{1/2},g_{1/2})\left[\sin^2(\varphi_+) + \frac{1}{3}\sin^2(\varphi_-)\right] + \rho^{\rm SS}(g_{-1/2},g_{-1/2})\left[\sin^2(\varphi_-) + \frac{1}{3}\sin^2(\varphi_+)\right]\Bigg) \\ &+2\eta^2\Delta s\Bigg({\rm Re}[\tilde{R}(g_{-1/2},g_{-1/2})]\left[\sin(\varphi_+)\cos(\varphi_+) - \frac{1}{3}\sin(\varphi_-)\cos(\varphi_-)\right] \\ &- {\rm Re}[\tilde{R}(g_{1/2},g_{1/2})]\left[\sin(\varphi_-)\cos(\varphi_-) - \frac{1}{3}\sin(\varphi_+)\cos(\varphi_+)\right]\Bigg)\ .\end{aligned} \tag{42}$$

In deriving this, we have neglected the steady-state populations of the excited levels, which are very small compared to the ground-level populations.

In view of (42), we now need to calculate $\tilde{R}(g_i,g_i)$ $(i = \pm 1/2)$. In order to do this, we first write the optical Bloch equations for the excited-state populations. For example, we have

$$\dot{\rho}(e_{3/2},e_{3/2}) = -\Gamma\rho(e_{3/2},e_{3/2}) - i\frac{\Omega}{\sqrt{2}}\cos(\varphi_+)[\rho(g_{1/2},e_{3/2}) - \rho(e_{3/2},g_{1/2})]. \tag{43}$$

As before, starting from this equation we have in steady state

$$\rho^{\rm SS}(e_{3/2},e_{3/2}) = s\cos^2(\varphi_+)\rho^{\rm SS}(g_{1/2},g_{1/2}), \tag{44}$$

where we have used (39). We also have

$$\begin{aligned}\tilde{R}(e_{3/2},e_{3/2}) &= \frac{1}{\Gamma - i\nu}\left[R^0(e_{3/2},e_{3/2}) - i\frac{\Omega}{\sqrt{2}}\cos(\varphi_+)[\tilde{R}(g_{1/2},e_{3/2}) - \tilde{R}(e_{3/2},g_{1/2})]\right] \\ &\simeq \frac{1}{\Gamma}\left[R^0(e_{3/2},e_{3/2}) - i\frac{\Omega}{\sqrt{2}}\cos(\varphi_+)[\tilde{R}(g_{1/2},e_{3/2}) - \tilde{R}(e_{3/2},g_{1/2})]\right],\end{aligned} \tag{45}$$

where for the last line we have used (33b). Inserting the results for the coherences [cf. (41)], the initial condition $R^0(e_{3/2},e_{3/2}) = \frac{\Omega}{\sqrt{2}}\sin[\varphi_+]\,\rho^{\rm SS}(g_{1/2},e_{3/2})$, and neglecting the excited populations, we find Eq. (45) becomes

$$\tilde{R}(e_{3/2},e_{3/2}) = is\sin(\varphi_+)\cos(\varphi_+)\rho^{\rm SS}(g_{1/2},g_{1/2}) + s\cos(\varphi_+)\tilde{R}(g_{1/2},g_{1/2}). \tag{46}$$

We now write the optical Bloch equations for the ground-state populations. For example, we have for $\rho(g_{1/2},g_{1/2})$

$$\dot{\rho}(g_{1/2},g_{1/2}) = \Gamma\left[\rho(e_{3/2},e_{3/2}) + \frac{2}{3}\rho(e_{1/2},e_{1/2}) + \frac{1}{2}\rho(e_{-1/2},e_{-1/2})\right] + \left[-i\frac{\Omega}{\sqrt{2}}\cos(\varphi_+)\rho(e_{3/2},g_{1/2}) + i\frac{\Omega}{\sqrt{6}}\cos(\varphi_-)\rho(e_{-1/2},g_{1/2}) + \text{c.c.}\right]. \quad (47)$$

Using the expressions for the optical coherences [cf. (39)] and the excited-state populations [cf. (44)], we see that in steady state

$$\rho^{\text{SS}}(g_{1/2},g_{1/2}) = \frac{\Gamma_{-\to+}}{\Gamma_{+\to-}+\Gamma_{-\to+}}, \quad (48)$$

where now

$$\Gamma_{\mp\to\pm} = \Gamma'\cos^2(\varphi_\pm). \quad (49)$$

Besides, taking the Laplace transform of (47), and using the results derived above, we find

$$-i\nu\tilde{R}(g_{1/2},g_{1/2}) = \Gamma_{-\to+}\tilde{R}(g_{-1/2},g_{-1/2}) - \Gamma_{+\to-}\tilde{R}(g_{1/2},g_{1/2}) + 2\Delta s\left[\sin(\varphi_+)\cos(\varphi_+) - \frac{1}{3}\sin(\varphi_-)\cos(\varphi_-)\right]\rho^{\text{SS}}(g_{1/2},g_{1/2}) + i\Gamma'\left[\sin(\varphi_+)\cos(\varphi_+)\rho^{\text{SS}}(g_{-1/2},g_{-1/2}) + \sin(\varphi_-)\cos(\varphi_-)\rho^{\text{SS}}(g_{1/2},g_{1/2})\right]. \quad (50)$$

This equation, together with that for $\tilde{R}(g_{-1/2},g_{-1/2})$ allows one to derive an analytic approximation to $\text{Re}[S(\nu)]$.

On the other hand, inserting the expression for the ground-level populations in steady state [cf. (48)] in the excited-state populations [cf. (44)] and substituting them in (32), we obtain for the diffusion constant D,

$$D = \frac{1}{5}\eta^2\Gamma s\frac{\cos^4(\varphi_+)+\cos^4(\varphi_-)+\frac{4}{9}\cos^2(\varphi_+)\cos^2(\varphi_-)}{\cos^2(\varphi_+)+\cos^2(\varphi_-)}. \quad (51)$$

Finally, we obtain for the coefficients $A_\pm$:

$$A_+(\nu) = A_-(-\nu) = \eta^2\frac{\Gamma s}{\cos^2(\varphi_+)+\cos^2(\varphi_-)}\left(\frac{8}{27}\frac{\Delta s\sin^2(\theta)f_1(\theta,\phi)}{\nu^2+(\Gamma_{+\to-}+\Gamma_{-\to+})^2}\left[\nu+\frac{2}{3}\Delta s f_1(\theta,\phi)\right]+f_2(\theta,\phi)\right), \quad (52)$$

where

$$f_1(\theta,\phi) = \cos(2\phi)[\cos(\theta)+\cos(2\phi)], \quad (53a)$$

$$f_2(\theta,\phi) = \cos^2(\varphi_+)\left[\sin^2(\varphi_+)+\frac{1}{3}\sin^2(\varphi_-)+\frac{2}{5}\cos^2(\varphi_+)+\frac{4}{45}\cos^2(\varphi_-)\right]+(\varphi_\pm\to\varphi_\mp). \quad (53b)$$

B. Cooling rate and final energy

Substitution of (52) as given by Eq. (52) into Eq. (28) shows that the minimum temperature occurs for $\Gamma' \ll \nu$. In this limit, it can be shown that the cooling rate (27) is

$$W = 8\eta^2\Gamma'\xi\frac{\sin^2(\theta)}{\cos^2(\varphi_+)+\cos^2(\varphi_-)}, \quad (54)$$

and the mean occupation number is

$$\langle n\rangle = -\frac{1}{2}+\xi+\frac{9}{16}\frac{f_2(\theta,\phi)}{\sin^2(\theta)}\frac{1}{\xi}, \quad (55)$$

where we have defined

$$\xi = -\frac{1}{3}\frac{\Delta s}{\nu}f_1(\theta,\phi). \quad (56)$$

Note that for $\theta = \pi/2$ and $\phi = 0$, Eqs. (54), (55), and (56) reduce to the expressions (23), (24), and (25), respectively.

V. DISCUSSION

In Sec. III, we have already given a qualitative explanation of the cooling mechanism in terms of the Sisyphus effect. Here, we present a more detailed discussion of the results derived in the preceding sections. All results presented below have been evaluated by the complete numerical solution of the problem introduced in Sec. II and are valid without restrictions (except for the Lamb-Dicke limit). However, the values were chosen close to parameters that are of experimental interest and can be calculated approximately with the analytical results above. In Figs. 3–10 shown below, the calculations according to

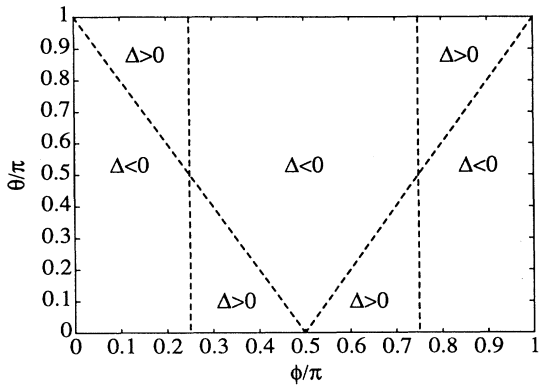

FIG. 3. Values of the parameters θ and ϕ indicating where cooling occurs for positive ($\Delta > 0$) and negative detunings ($\Delta < 0$). This plot is based on formulas derived in Sec. IV A, which are valid under the conditions $s \ll 1$, $\nu \ll \Gamma, \Delta$.

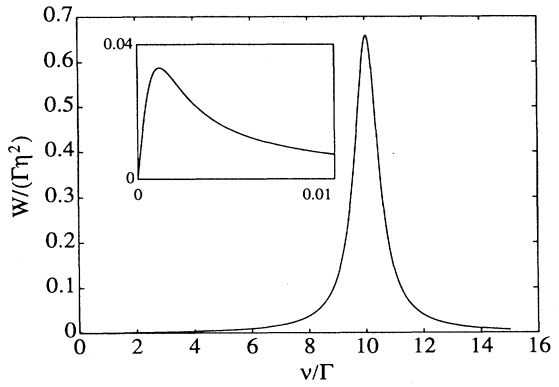

FIG. 4. Cooling rate W in units of $\Gamma\eta^2$ as a function of the trap frequency ν. Parameters: $\Omega = \Gamma$, $\Delta = -10\Gamma$, $\theta = \pi/2$, $\phi = 0$. The inset shows the region $0 \leq \nu/\Gamma < 0.01$ on an expanded scale.

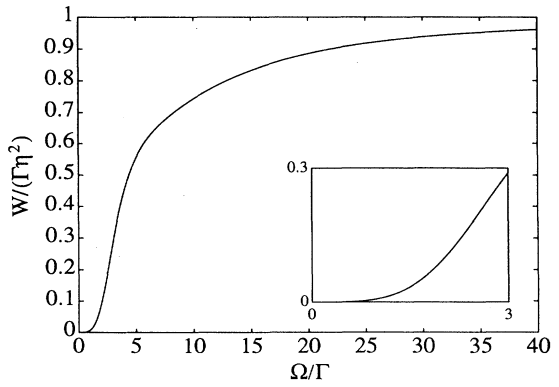

FIG. 5. Cooling rate W in units of $\Gamma\eta^2$ as a function of the Rabi frequency Ω. Parameters: $\nu = 0.01\Gamma$, $\Delta = -10\Gamma$, $\theta = \pi/2$, $\phi = 0$. The inset shows the small-Ω dependence on a larger scale.

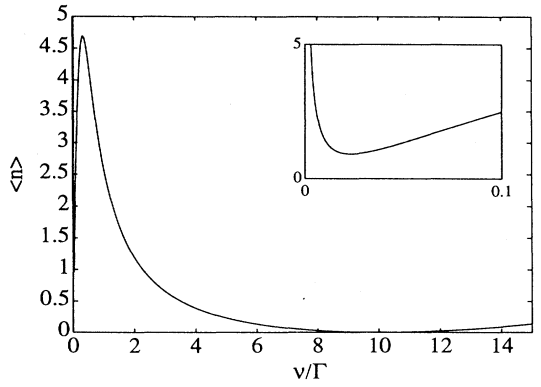

FIG. 6. Final quantum number $\langle n \rangle$ as a function of the trap frequency ν. Parameters are the same as in Fig. 4. The inset shows the small-ν dependence on a larger scale.

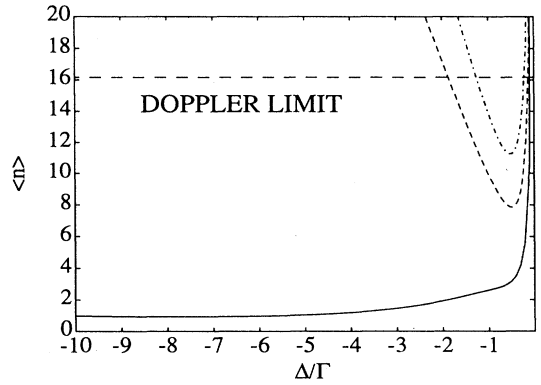

FIG. 7. Final quantum number $\langle n \rangle$ as a function of negative detuning Δ for $\nu = 0.03\Gamma$, and $\Omega = \Gamma$. Solid line: polarization gradient cooling ($\theta = \pi/2$, $\phi = 0$). Short dashes: cooling at the node of a standing wave ($\theta = 0$, $\phi = \pi/2$). Dashed-dotted line: cooling at the point of maximum gradient in a standing wave ($\Omega = 0.1\Gamma$, $\theta = 0$, $\phi = \pi/4$). The long-dashed line indicates the Doppler limit.

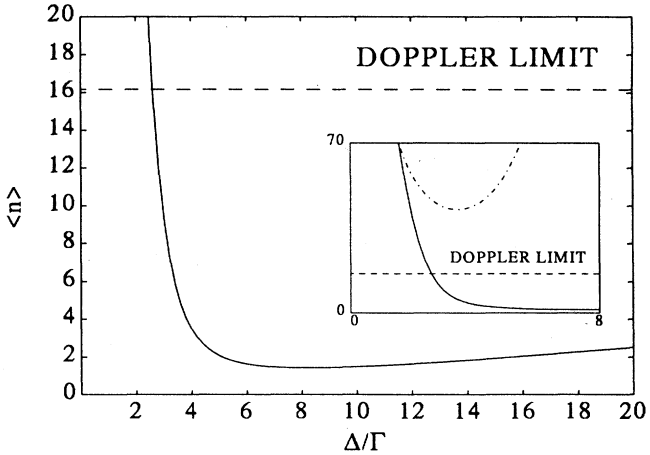

FIG. 8. Final quantum number $\langle n \rangle$ as a function of positive detuning Δ for $\nu = 0.03\Gamma$, $\Omega = 3\Gamma$, $\theta = \pi/4$, and $\phi = \pi/3$. Inset: Solid line as in main figure, dashed-dotted line shows the result at the point of maximum gradient in a standing wave ($\Omega = 0.1\Gamma$, $\theta = 0$, $\phi = \pi/4$). The dashed line indicates the Doppler limit.

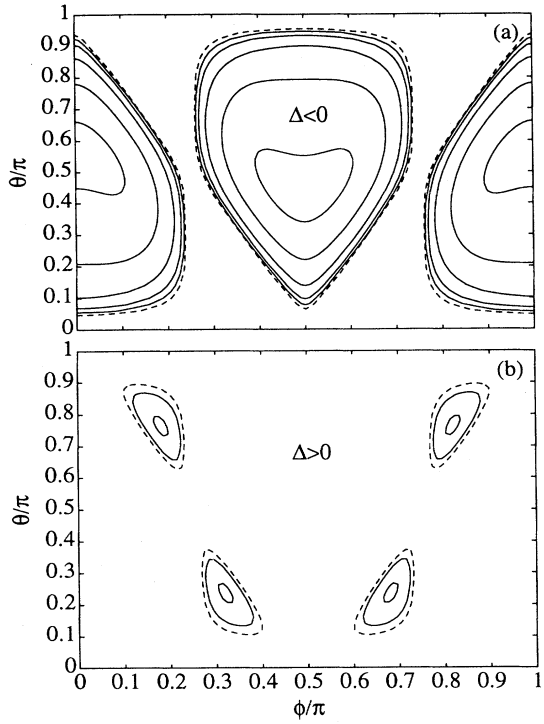

FIG. 9. Contour plot of the final quantum number $\langle n \rangle$ as a function of θ and ϕ. Parameters are $\Omega = \Gamma$, $\nu = 0.023\Gamma$ and (a) $\Delta = -10\Gamma$, and the solid lines represent $\langle n \rangle = 1, 2, 5, 10, 15$, (b) $\Delta = 10\Gamma$ and the solid lines represent $\langle n \rangle = 10, 15$. In (a) and (b) the dashed lines indicate the Doppler limit given by $\nu(\langle n \rangle + 1/2) = \Gamma/2$ (in this case $\langle n \rangle \simeq 21$).

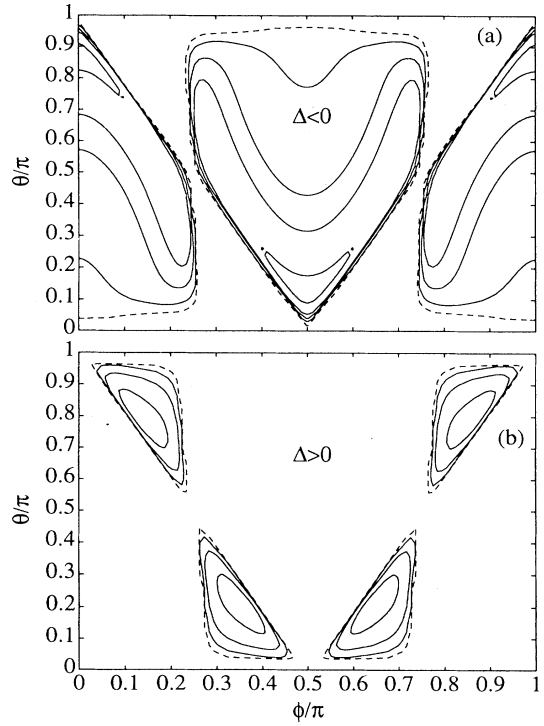

FIG. 10. Same as in Fig. 9 with parameters $\Omega = 3\Gamma$, $\nu = 0.03\Gamma$, and (a) $\Delta = -6\Gamma$, and the solid lines represent $\langle n \rangle = 1, 3, 5, 10, 15$, (b) $\Delta = 6\Gamma$ and the solid lines represent $\langle n \rangle = 3, 5, 10$. In (a) and (b) the dashed lines indicate the Doppler limit given by $\nu(\langle n \rangle + 1/2) = \Gamma/2$ (in this case $\langle n \rangle \simeq 16.6$).

the analytical formulas presented above agree with the numerical solutions.

According to expressions (54) and (55) derived above, the cooling rate and final energy do not change if we substitute $\theta \to -\theta$, or $\phi \to \phi + \pi$. Thus we will restrict the treatment to angles $0 \leq \theta, \phi \leq \pi$.

A. Cooling rates

Cooling occurs for positive cooling rates ($W > 0$). In view of (54), this condition is equivalent to $\xi > 0$. Hence, cooling exists for positive and negative detunings, depending on the values taken on by θ and ϕ [see (56)]. Figure 3 shows the areas in a ϕ–θ plane where cooling occurs for negative, or "red" detunings (indicated as $\Delta < 0$ in the figure) and for positive, or "blue" detunings (indicated as $\Delta > 0$). Note first that for $\theta = \pi/2$ (which corresponds to the lin $\perp$ lin laser configuration) cooling occurs only for negative detunings. In contrast, for $\theta = 0$, i.e., when the lasers form a linearly polarized standing wave, there is no Sisyphus-cooling mechanism ($W = 0$) [18]. The reason for this behavior is that in this case the two potentials $U_\pm$ coincide, and therefore there is no Sisyphus effect. For a given angle θ, if $\phi = \pi/4$ or $\phi = 3\pi/4$, the cooling rate is also zero, as can be seen from definitions in Eqs. (54), (56), and (53a). As mentioned in Sec. III, in this case the potentials $V_\pm$ are centered at the same point in space, and therefore no net energy transfer can take place in a cycle of Raman transitions ($|g_{1/2}\rangle \to |g_{-1/2}\rangle \to |g_{1/2}\rangle$). As a consequence, there is only heating due to diffusion, and accordingly Sisyphus cooling is not possible. This situation corresponds, for example, to the antinodes of the two potentials $U_\pm$ of Fig. 2.

On the other hand, it can be easily shown from (54) that the cooling rate is maximum (that is, cooling is most effective) for $\theta = \pi/2$ and $\phi = 0$, as considered in the semiclassical treatment. This is in contrast to what occurs for a neutral atom, where there is always a certain angle $\theta \neq \pi/2$ that maximizes the friction force [11].

Below we show that minimum temperatures are found for $\xi \approx 1$, which gives a cooling rate $W \approx \eta^2\Gamma' \ll \Gamma' = \Gamma s2/9$, i.e., many Raman transitions must occur for an appreciable reduction of the ion energy. On the other hand, with this technique cooling below the Doppler limit is possible, and we therefore consider the cooling rate in more detail. In Fig. 4 the cooling rate is shown as a function of ν/Γ. This figure is to be compared with a similiar figure in Ref. [9] (cf. Fig. 7 of Ref. [9]) in which the friction force (for neutral atoms) due to cooling with polarization gradients is drawn as a function of the velocity. For a trapped ion we use the trap frequency ν instead. Figure 4 has been evaluated for the following parameters:

$\Delta = -10\Gamma$, $\Omega = \Gamma$, $\phi = 0$, and $\theta = \pi/2$. As can be seen from Fig. 4, there is a large maximum next to a trap frequency $\nu = -\Delta$. This corresponds to the well-known sideband cooling regime, i.e., $\Gamma \ll \nu$, where cooling is achieved via optical pumping between the different levels of the trap potential, hence the high cooling rate. As the inset shows, for very low trap frequencies $\nu \ll \Gamma$ there is an enhanced cooling rate due the polarization gradients. The trap frequency at which the maximum appears is determined by the interplay between cooling and heating by the diffusion processes. For these parameters, very low temperatures are achieved eventually, even in the weak-confinement limit.

We note that the cooling rate is proportional to Ω^4, as can be deduced from (54). This behavior is shown in Fig. 5 in which the cooling rate is drawn as a function of the Rabi freqency Ω for parameters as in Fig. 4 and with a trap frequency $\nu = 0.01\Gamma$. The physical reason for this Ω^4 dependence can be explained as follows: the separation between the potentials $V_\pm$ for a fixed position z, that is, $V_+(z) - V_-(z)$, as indicated in Fig. 2 is proportional to Ω^2 [see Eq. (11)]. So, in each Raman transition from $|g_{\pm 1/2}\rangle$ to $|g_{\mp 1/2}\rangle$ the energy changes in a quantity proportional to Ω^2. On the other hand, the rate at which these transitions occur is again proportional to Ω^2 [see Eq. (8a)]. The inset in Fig. 5 shows the cooling rate for small Rabi frequencies, which are clearly to be preferred in order to obtain small final energies (small diffusion). This Ω^4 dependence is only present when the ion is confined to dimensions smaller than the optical wavelength. For free atoms that are moving in space, the friction force has to be averaged over many wavelengths and therefore the Ω dependence disappears due to the counterproductive terms present at the antinodes. Thus in semiclassical Sisyphus cooling of neutral atoms the friction force is essentially independent of the laser intensity for low velocities, i.e., at the last stages of the cooling process [9]. In contrast, the present situation in the ion trap is reminiscent of laser cooling of quantized optical molasses in a lin $\perp$ lin configuration [19–22]. For $J_g = 1/2 \rightarrow J_e = 3/2$ atom (Fig. 1) one finds cooling to the ground states of the *optical potentials* $U_\pm(z)$ (compare Fig. 2). Note that the bottoms of the potential wells $U_\pm(z)$ coincide with the points of pure $\sigma^\pm$–polarized light. Since the vibrational ground state in the optical potential (of dimension a) is well localized on the scale of a wavelength λ, interpotential transitions $U_+(z) \leftrightarrow U_-(z)$ are proportional to $\eta_m^2 \Gamma'$ with Lamb-Dicke parameter $\eta_m = \pi a/\lambda \ll 1$ (Lamb-Dicke narrowing). This is in contrast to the case of the ion trap where confinement to the Lamb–Dicke limit is due to the trapping potential.

B. Final energies

The final state of the external degrees of freedom follows a Bose-Einstein distribution, with mean quantum number given in (55). According to (28) the final energy reached by the ion is

$$E^{\mathrm{SS}} = \nu \left[\xi + \frac{9}{16} \frac{f_2(\theta,\phi)}{\sin^2(\theta)} \frac{1}{\xi} \right]. \tag{57}$$

As mentioned in Sec. III, the first term is related to the possible heating due to the change in the potential energy when the ion switches between the two potentials, while the second is related to heating due to diffusion of the scattering force and the dipole force. For $\theta = \pi/2$ and $\phi = 0$ this expression coincides with (24), showing that the semiclassical treatment is completely valid in the limits considered here. The reasons for this coincidence have been discussed in [6].

It can be easily shown that the minimum energy is found when

$$\xi = \frac{3}{4} \frac{\sqrt{f_2(\theta,\phi)}}{|\sin\theta|}, \tag{58}$$

resulting in

$$\langle n \rangle_{\min} = \frac{3}{2} \frac{\sqrt{f_2(\theta,\phi)}}{\sin^2(\theta)} - \frac{1}{2}. \tag{59}$$

For $\theta = \pi/2$ and $\phi = 0$ this gives $\langle n \rangle_{\min} = 0.93$, which corresponds to a thermal distribution with populations in the ground and first excited levels of 51% and 25%, respectively. The minimum energy is found in the limits $\theta \rightarrow \pi$ and $\phi \rightarrow 0$, resulting in $\langle n \rangle_{\min} = 0.72$, which corresponds to populations of 58% and 24% in the ground and excited levels, respectively.

Figure 6 shows the final energy, given by the final quantum number $\langle n \rangle$, as a function of the trap frequency ν with the same parameters as in Fig. 4. Clearly, the minimum value is reached for the sideband cooling limit (i.e., $\langle n \rangle \rightarrow 0$ at $\nu = -\Delta$). The polarization gradient cooling shows up for the weak-confinement region $\nu \ll \Gamma$ and a minimum of the energy is reached with about $\langle n \rangle \simeq 1$ (cf. inset in Fig. 6).

In order to compare the final energies obtainable with different cooling techniques for a trapped ion, we have drawn in Fig. 7 the final energies (in terms of the quantum number $\langle n \rangle$) as a function of the detuning. The parameters are $\Gamma = 1$, $\Omega = \Gamma$, $\nu = 0.03\Gamma$, i.e. we investigate the weak-confinement case, which is of importance for most experiments. The solid line shows the result for polarization gradient cooling as obtained with the lin $\perp$ lin configuration, i.e., $\phi = 0$ and $\theta = \pi/2$. The short dashes indicate a calculation for laser cooling of the same ion placed at the node of a standing-wave field [7] for the same parameters, but $\phi = \pi/2$ and $\theta = 0$. The dashed-dotted curve shows a calculation for the ion placed at the point of the maximum gradient in a standing wave, i.e., $\phi = \pi/4$ and $\theta = 0$. The results found in the last two curves do not appreciably differ from those obtained for simple two-level systems. Note that the latter curve was evaluated with a Rabi frequency $\Omega = 0.01$, which shows the same results as a traveling wave would give [7]. The long dashes indicate the Doppler limit $\langle n \rangle = \Gamma/(2\nu) - 1/2$. Note that in the low-intensity limit the lowest final energy reached by a two-level system in a traveling wave is more correctly given by $\Gamma(1+\alpha)/4$ where α takes the radiation pattern into account. Usually, for one-dimensional treatments, $\alpha = 1$ (hence the Doppler limit); for more realistic calculations, including the dipole radiation pattern as considered in this paper,

$\alpha < 1$ (e.g., for a $m_J = 1/2 \rightarrow m_J = 3/2$, $\alpha = 2/5$). Hence for the system introduced in Sec. II the dashed-dotted result shows a minimum value slightly less than the Doppler limit. As known for laser cooling an ion at the node of a standing-wave field, the minimum energy is about half the Doppler limit. However, the detuning range for which the minimum energy is reached is very restricted. This is not the case for the polarization gradient cooling as is clearly visible from Fig. 7. In fact, the minimum energy occurs at a detuning of about $\Delta = -8\Gamma$, in agreement with the expected value from Eq. (55).

Note that the results in Fig. 7 show the behavior for detunings below the resonance, i.e., for negative or "red" detunings. As was stated above, polarization gradients allow cooling of a trapped ion also for positive, i.e., blue detunings. This is shown in Fig. 8 where the final kinetic energy is drawn as a function of the detuning with the following parameters: $\Omega = 3\Gamma$, $\nu = 0.03\Gamma$, and with angles $\theta = \pi/4$ and $\phi = \pi/3$. Again, the minimum value for $\langle n \rangle$ is about 1 and much below the Doppler limit, which is indicated by the dashed line. The inset shows a comparison of the cooling with polarization gradients and pure intensity gradients (i.e., cooling of an ion placed at the point of maximum gradient in a standing wave) for which the result is given by the dashed-dotted line. Note that again the final energy does not depend in a sensitive way on the detuning of the laser.

To show the dependence of the cooling and the final energy as a function of the angles θ and ϕ, we have plotted in Fig. 9 the minimum energy given by $\langle n \rangle$, for negative detunings $\Delta < 0$ [Fig. 9 (a)] and for positive detunings $\Delta > 0$ (Fig. 9(b)]. Parameters for this figure are $\Omega = \Gamma$, $\nu = 0.01\Gamma$, and $\Delta = \pm 10\Gamma$. The solid lines in the plots show lines of equal quantum number $\langle n \rangle$; in Fig. 9(a) the lines represent $\langle n \rangle = 1, 2, 5, 10, 15$ and in Fig. 9(b) at $\langle n \rangle = 10, 15$. The Doppler limit at $\langle n \rangle = 21$ is given by the dashed line. This figure demonstrates that cooling to very low temperatures is possible for wide ranges of the angles θ and ϕ. Thus, in particular for negative detunings, laser cooling of trapped ions with polarization gradients should be fairly insensitive to misalignments of the standing-wave arrangement. This is confirmed by a calculation for a different set of parameters ($\Gamma = 1$, $\Omega = 3\Gamma$, $\nu = 0.03$, and $\Delta = \pm 6\Gamma$) and is shown in Fig. 10. Solid lines in Fig. 10(a) show values of $\langle n \rangle = 1, 3, 5, 10$ and in Fig. 10(b) $\langle n \rangle = 3, 5, 10$. The Doppler limit is indicated by the dashed lines at $\langle n \rangle = 16.6$. Note that cooling below the Doppler limit is possible almost at any set of parameters ϕ and θ except for very narrow regions, indicated by the straight lines in Fig. 3.

Finally, an alternative explanation for the cooling mechanism discussed in Sec. II should be mentioned. As we have discussed elsewhere, laser cooling of a trapped ion can only be accomplished when the classical absorption-gain coefficient for three-wave mixing is asymmetric with respect to the laser carrier frequency [7]. For two-level atoms, this is usually achieved by choosing a negative detuning, and in this case, the final energy is always limited by the width of the central peak in this absorption coefficient. However, with the Zeeman structure considered here, the width of the central peak can be very small (it is of the order of Γ'). Asymmetric absorption is achieved in this case by the choice of the angles θ and ϕ and hence cooling occurs.

VI. CONCLUSION

Laser cooling of a trapped ion with polarization gradients was theoretically investigated in the Lamb-Dicke limit and for a $J_g = 1/2 \rightarrow J = 3/2$ transition. The problem was treated numerically and allowed us to calculate final energies and cooling rates of general validity. Analytic expressions for the final energy and the cooling rates were derived using a semiclassical treatment and assuming that the rate for optical pumping between the ground states is the smallest time constant in the system. These expressions completely agree with analytic results obtained from a full quantum treatment of the system. The results show that laser cooling of trapped ions using polarization gradients leads to final energies of about $\langle n \rangle = 1$, which is well below what would otherwise be expected for the weak-binding case. Of utmost experimental importance is the fact that the results are insensitive to the precise position of the ion within the laser configuration and to the detuning of the cooling laser. Therefore, this technique is ideally suited for achieving lowest temperatures with single trapped ions in the weak-confinement regime. Note that the numerical values used for all figures are realistic and very close to numbers that are encountered, e.g., with Be^+ and Mg^+ ions, which have the level scheme as indicated in Fig. 1. The calculations also are readily applicable to experiments with Ba^+, Ca^+, Sr^+, Hg^+, and Yb^+ ions, which are currently being investigated in experiments on quantum optics, and for time and frequency standard applications. In conclusion, we perceive good potential for this technique to facilitate laser cooling of trapped ions to the ground state without the need for strong confinement, either using weak transitions or sophisticated trap technology.

ACKNOWLEDGMENTS

J.I.C and R.B. acknowledge travel support from NATO. R.B. is supported in part by the Deutsche Forschungsgemeinschaft. The work at JILA is supported in part by the National Science Foundation.

[1] D.J. Wineland, W.M. Itano, and R.S. VanDyck, Jr., Adv. At. Mol. Phys. **19**, 135 (1983).

[2] P.E. Toschek, in *New Trends in Atomic Physics*, Proceedings of the Les Houches Summer School, Session XXXVIII, edited by G. Grynberg and R. Stora (North-Holland, Amsterdam 1984), Vol. 1, p. 381.

[3] R. Blatt, in *Fundamental Systems in Quantum Optics*, Proceedings of the Les Houches Summer School, Session

LIII, edited by J. Dalibard, J.M. Raymond, and J. Zinn-Justin (Elsevier, Amsterdam, 1992), p. 253.
[4] See, e.g., special issue on *The Physics of Trapped Ions*, edited by R. Blatt, P. Gill, and R.C. Thompson, J. Mod. Opt. **39**, 192 (1992).
[5] See articles in *Laser Cooling and Trapping*, J. Opt. Soc. Am. B **6** (1989).
[6] D.J. Wineland, J. Dalibard, and C. Cohen-Tannoudji, J. Opt. Soc. Am. B **9**, 32 (1992).
[7] J.I. Cirac, R. Blatt, P. Zoller, and W.D. Phillips, Phys. Rev. A **46**, 2668 (1992).
[8] J. Dalibard and C. Cohen-Tannoudji, J. Opt. Soc. Am. B **2**, 1707 (1985).
[9] J. Dalibard and C. Cohen-Tannoudji, J. Opt. Soc. Am. B **6**, 2023 (1989).
[10] P.J. Ungar, D.S. Weiss, E. Riis, and S. Chu, J. Opt. Soc. Am. B **6**, 2058 (1989); D.S. Weiss, E. Riis, Y. Shevy, P.J. Ungar, and S. Chu, *ibid.* **6**, 2072 (1989).
[11] V. Finkelstein, P.R. Berman, and J. Guo, Phys. Rev. A **45**, 1829 (1992).
[12] D.J. Wineland and W.M. Itano, Phys. Rev. A **20**, 1521 (1979); W.M. Itano and D.J. Wineland, *ibid.* **25**, 35 (1982).
[13] S. Stenholm, Rev. Mod. Phys. **58**, 699 (1986).
[14] M. Lindberg and S. Stenholm, J. Phys. B **17**, 3375 (1985).
[15] M. Lindberg and J. Javanainen, J. Opt. Soc. Am. B **3**, 1008 (1986).
[16] F. Diedrich, J.C. Bergquist, W.M. Itano, and D.J. Wineland, Phys. Rev. Lett. **62**, 403 (1989).
[17] J.P. Gordon and A. Ashkin, Phys. Rev. A **21**, 1606 (1980).
[18] Note that our discussion is based on the approximations $s \ll 1$, $\nu \ll \Gamma, \Delta$. We expect Doppler cooling to occur; however, in the limits $\Delta > \Gamma > \nu$, the final energy (given approximately by $\Delta/4$) will be very high.
[19] P. Verkerk, B. Lounis, C. Salomon, C. Cohen-Tannoudji, J.Y. Courtois, and G. Grynberg, Phys. Rev. Lett. **68**, 3861 (1992).
[20] P.S. Jessen, C. Gerz, P.D. Lett, W.D. Phillips, S.L. Ralston, R.J.C. Spreeuw, and C.I. Westbrook, Phys. Rev. Lett. **69**, 49 (1992).
[21] Y. Castin and J. Dalibard, Europhys. Lett. **14**, 761 (1991).
[22] P. Marte, R. Dum, R. Taïeb, and P. Zoller, Phys. Rev. A **47**, 1378 (1993); P. Marte, R. Dum, R. Taïeb, P. Lett, and P. Zoller (unpublished).